Design Wind Loads for Wind Power Applications

WINDPOWER 2008

Jon A. Peterka, PhD, P.E.

Kirsten Orwig, MS

Rick Damiani, PhD, P.E. (Europe)

Brad Cochran, MS

CPP, Inc.

1415 Blue Spruce Drive

Fort Collins, CO 80524

Corresponding Author: Jon Peterka

970-221-3371

jpeterka@cppwind.com

Design Wind Loads for Wind Power Applications

Introduction

The survival in design-level wind events and fatigue loading of wind turbines and other wind farm structures is an integral part of wind power economics. The design of fatigue-sensitive structures is not well represented by building code approaches. However, aspects of wind code approaches along with well-established wind engineering practices can be used to define design wind events and provide guidance to safe design procedures. This paper shows how extreme wind events can be quantified based on these techniques. The methods are extended further to transfer the events from the location of historical measurements to wind power sites. The impact of ordinary straight line winds, hurricanes, and tornados on wind turbines is included.

Wind Speed Design Concepts

Design wind speeds are typically defined in building codes as 50-year events, except in hurricane (also called typhoons or tropical cyclones) prone regions. In these regions, different recurrence intervals are often used to ensure that structural reliability is similar to that in non-hurricane regions. The US national wind load standard and the International Building Code that references it (ASCE 7 and IBC, respectively) permit use of a Load Resistance Factor Design (LRFD). LRFD is based on a "strength design point," which is the structure's first yield at a roughly 700 year event. Figure 1 shows that the rate of increase of wind speed with recurrence interval for hurricanes is higher than it is for non-hurricane winds. A hurricane requires an effective load factor of 2.0 to cause first yield at a 700 year recurrence interval (red curve), while in non-hurricane regions a load factor of 1.6 is required (blue curve). The hurricane wind map values in ASCE 7 and IBC have both been adjusted to a value of V(700)/√1.6 to reflect greater load factors/shorter recurrence intervals for hurricane regions. Here V(700) is the gust wind speed at 10 m in open country exposure for a return period of 700 years.

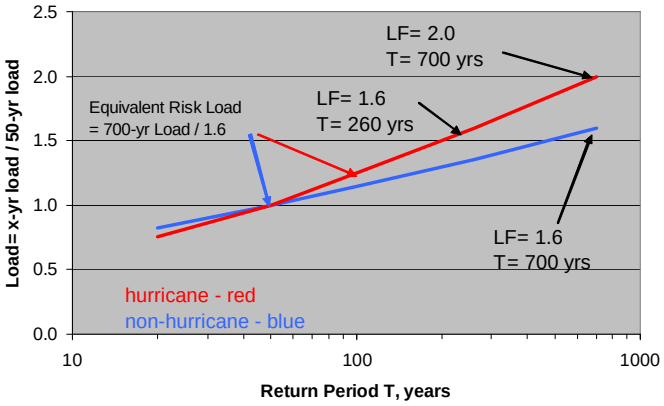

Figure 1: Equivalent Risk Design in ASCE 7.

The recurrence interval of 700 years selected for the LRFD strength design point for building structures in the US is not necessarily the proper one for use in wind power applications. This return period was determined by life-safety issues in occupied buildings. If it

could be arranged that no personnel would be in a wind power field at the time of high-risk storms, then the strength design point could be selected only on the basis of economics. While this might be possible for straight-line winds and hurricanes, it is not as simple for thunderstorms whose outflows can travel long distances from the storm and increase to the maximum speed with rise times of much less than a minute.

The time duration of the design wind speed is important because the ratio of peak-to-mean (gust factor) differs between storm types. For straight line winds, the gust factor averages about 1.5-1.6 at 10 m in an open country exposure. Thunderstorms generate their high winds from downbursts that spread laterally on the ground. The gust factor for thunderstorms is highly variable and can easily range from 1.5 to 4.0 or more. At design wind speeds of 40 – 51 m/s (90 – 114 mph) representing 50 to 700 year speeds in the 90 mph zone on the ASCE 7-05 wind map, a gust with 3-second duration will travel 120 – 150 m (400 – 500 ft), fully encompassing most structures, and is thus reasonable to use for load definition. If a longer time average is used, then a factor must be included to transfer the wind speed to a short duration gust – a factor that is different for different storm types – which is undesirable and difficult to implement in design calculations.

In using measured wind speeds to define design level wind speeds, long historical records of more than 20 years are needed (and more than 100 is desirable) to limit uncertainties in defining the design wind speeds and recurrence intervals for non-hurricane regions. Figure 2 shows the standard deviation of sampling error, the uncertainty of the true recurrence interval wind speed, as a function of the number of years of record taken from Peterka and Shahid, 1998. Sampling error decreases as $1/\sqrt{N}$, where N is the number of years of record. At wind power sites where short records are taken in order to include the amplification of ambient winds by terrain, a 1 – 5 year record will produce an uncertainty of 10-20 percent in wind speed (20-40 percent in load). This is too large for economic assessment of wind loads for structural purposes. Some correlation to regional historic wind speed records is needed to limit statistical sampling error and to account for multi-decadal variability that is often seen in atmospheric phenomena.

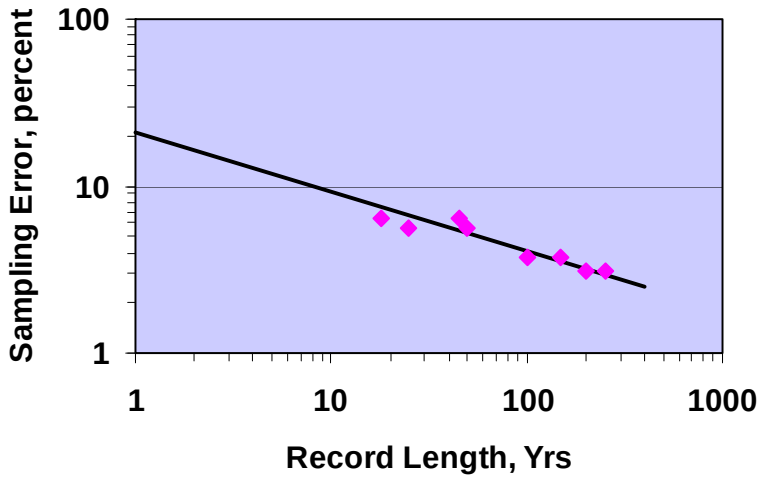

Figure 2: Sampling Error Standard Deviation. Data from Peterka and Shahid, 1998; line shows $1/\sqrt{N}$ functional fit to data.

Historical meteorological stations with long records can sometimes be combined into "superstations" (Peterka and Shahid, 1998) to obtain effective records of more than 100 years. A "superstation" is a collection of meteorological stations in a region of similar wind climatology whose wind speed records are statistically independent. Record lengths less than 5 years can lead to standard deviations of sampling error in wind speed in the 15-20 percent range (Peterka and Shahid, 1998), as shown in Figure 2. This type of regional wind speed analysis has already been performed for the continental US, and is available in the ASCE 7 wind map. Updates should be performed for specific projects, since there is more data available now than when the map was developed (peak gust data available through 1990). It should be noted that peak gust data for the US Automated Surface Observation System (ASOS), beginning in the mid 1990s for many locations, is different than that recorded earlier. The earlier gust was the daily peak on a strip chart recording, while the ASOS 5-seocnd gust is the largest daily value of a running average of 5 one-second measurements. The ASOS gust data must be evaluated prior to including them in the 3-second gust record. For other areas of the world, varying levels of analysis have been used; a review, and in many areas a re-evaluation, of design wind speed is required. For structures that have different load sensitivities to wind directions, the wind direction attached to wind records must be included in the analysis.

An example of an analysis for design wind speed produced for this paper is a site within the US Great Plains wind power producing area, shown in Figure 3. It is a superstation comprised of 5 stations in South Dakota and Nebraska. It was selected to demonstrate (but not resolve) some of the issues that complicate the analysis. Figure 3a shows maximum yearly peak gust speeds as measured at the various sites corrected to 10 m elevation using the same method as Peterka and Shahid (1998). The data include the older 2-3 second gust records, and the newer Automated Surface Observation System (ASOS) 5-second gusts corrected to 2-3 second gusts using Figure C6-4 of ASCE 7-05. Note the apparent decrease in speed with time. No effort was expended to understand this potential trend for this case, but a full analysis would assess this issue.

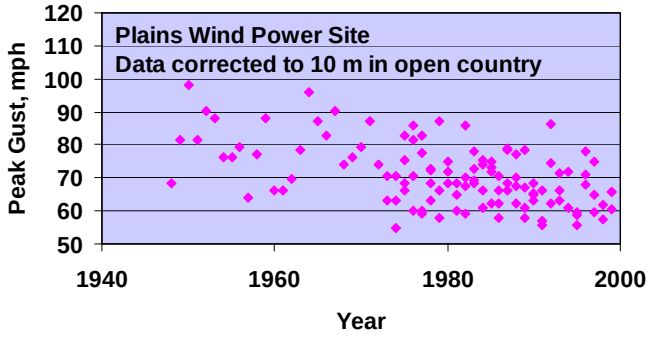

Figure 3a: Time series of yearly maximum wind speeds.

Figure 3b shows a Type I Extreme Value Distribution fit to the 117 station-years of data from Figure 3a. The 50-year return period gust speed from this analysis is 93 mph in comparison to 90 mph for this region of the ASCE 7 map (Peterka and Shahid, 1998). This 3 mph difference is less than one standard deviation of sampling error of 3.4 mph determined by Peterka and Shahid (1998) for this record length. Because of regional consistency of wind speeds, a 50-year

speed of 90 mph could be used. The wind speed corresponding to the 700-year recurrence interval strength design point of an LRFD analysis is 111 mph (with a slope vs. return period that gives a slightly lower speed than ASCE 7-05 of 90√1.6 = 114 mph).

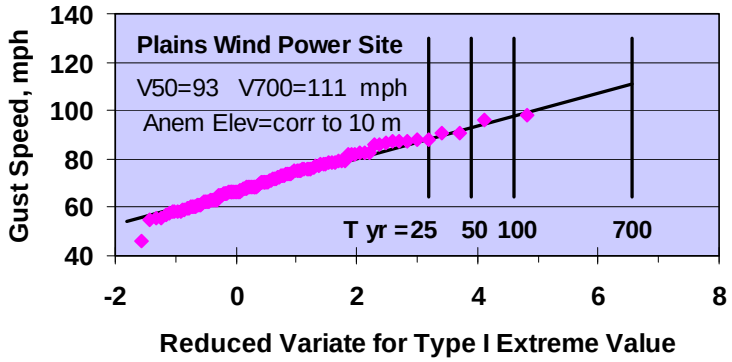

Figure 3b: Type I analysis of Superstation wind speeds.

Transfer of the design event from historical measurement sites to wind power sites is considered for two situations. First, if the ground surface roughness, as described by the effective roughness length Zo, is different at the turbine site than at the historical measurement site, then a roughness change algorithm should be implemented, see for example ESDU (1993a,1993b) and Figure 4a. In this analysis, a new internal boundary layer compatible with the new ground roughness begins to grow downwind of the change in roughness, and will become the atmospheric boundary layer after a number of kilometers. A series of roughness changes in close proximity means that the velocity vertical profile is a combination of many upwind profiles, and may not fit well to the power law profile assumed for many wind power sites.

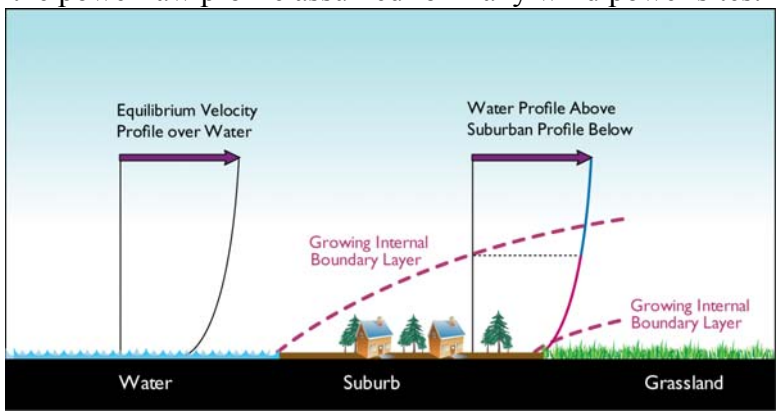

Figure 4a: Schematic of wind flow over surface roughness change.

The second situation is where the wind power site is in complex terrain where amplification of wind is significant (the primary reason most wind power sites are selected). For very simple terrain such as the crest of a 2-dimensional escarpment or an isolated, symmetrical 3-dimensional hill, guidance is provided in ASCE 7. For more complicated terrain, recourse to a small-scale terrain model in a wind tunnel designed to model the atmospheric boundary layer is the most accurate way to assess the wind speedup. An example is shown in Figure 4b. In this figure, an atmospheric boundary layer scaled to the model scale is developed by the spires, barrier, and distributed roughness over about 16 m (55 ft) in the long test section of the wind

tunnel. The vertical profile of mean velocity and turbulence appropriate to the upwind area for a neutrally stable atmospheric wind flow is established [see Cermak (1971, 1975) for details and validation of this method, and ASCE (1999) for test requirements]. At the speeds for design of structures, the wind flow is dominated by mechanical turbulence, and is thus neutrally stable. Measurement probes are available to measure all three components of mean velocity and all components of the turbulence shear stress matrix.

Figure 4b: Terrain model in a boundary layer wind tunnel.

Most of the highest wind speed gusts recorded east of the Rocky Mountains in the US are due to thunderstorms. Thunderstorm outflows occur as air descends in a thunderstorm and spreads laterally across the ground. The structures of thunderstorm outflows are different from straight line winds in that they reach a peak at 30 – 200 m above the surface. Figure 5, from Chay (2006), shows the progression of a single realization of a computer simulation of a thunderstorm outflow. The important information to glean from this figure is that outflows have a peak wind speed at roughly the hub height of wind turbines and changes with time and space. Thus the power law shear index commonly used for turbine survival winds is not correct for many of the design level wind speeds encountered. It should be emphasized that statistics of thunderstorm outflow vertical profiles is not yet quantified due to the highly transient nature of these events. Orwig and Schroeder (2007) further demonstrate some problems with using traditional statistical methods for analyzing thunderstorm outflows.

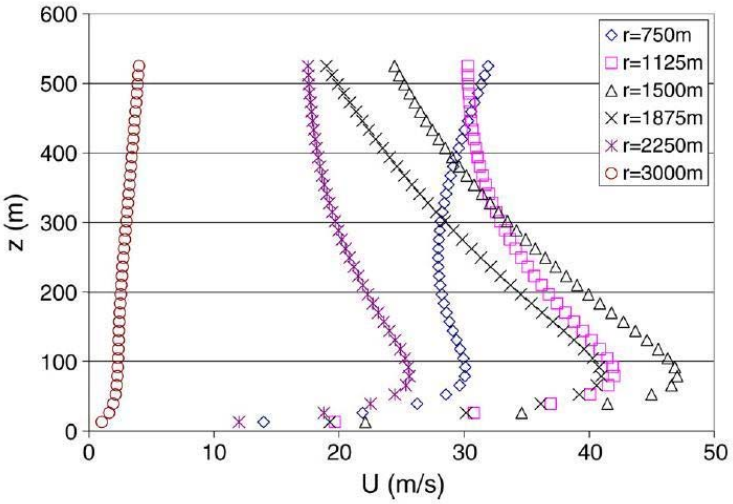

Figure 5: Progression of thunderstorm outflows using a numerical simulation (from Chay et al., Engr. Structures, 2006).

Hurricane (Typhoon, Cyclone) Design Speeds

In many areas, historical wind records are insufficient to define design-level hurricane wind speeds. On the US Atlantic and Gulf of Mexico coasts, there are very few measurements of peak hurricane wind speeds present in the historic record. Power outages (with no battery backup), anemometer vulnerability to debris, and meteorological tower structural failures have prevented strong maximum gusts from appearing in the record. There are some locations with sufficient measurements to use historical data – for example, Guam has a usable record (not currently digitized), and Taiwan has some historical digital and paper records that do not appear to be fully consistent.

In the past few years good data from US Atlantic and Gulf offshore buoys have been obtained, and dropsondes (disposable sensors dropped from airplanes in hurricanes) have provided some useful data, but insufficient to predict hurricane design speeds from measured data.

ASCE 7 does not permit design wind speeds in hurricane prone areas of the US to be determined from historical measurements of wind speeds at a meteorological station. ASCE 7-05 says, "In hurricane-prone regions, wind speeds derived from simulation techniques shall only be used in lieu of the basic wind speeds given in Fig. 6-1 [of ASCE 7-05] when … approved simulation and extreme value statistical analysis procedures are used (the use of regional wind speed data obtained from anemometers is not permitted to define the hurricane wind-speed risk along the Gulf and Atlantic coasts, the Caribbean or Hawaii) …"

The technology currently used to determine design hurricane wind speeds is to employ Monte Carlo methods to simulate a long history of storms from measured statistics of their physical properties such as central pressure, radius of maximum winds, and other variables (Vickery et al., 2000a, 2000b; Twisdale and Vickery, 1993; Banks and Peterka, 2001; Peterka and Banks, 2002). In this approach, entire hurricane tracks are generated by a random walk method in which changes (at uniform time intervals) in speed of the storm along the track,

change in direction, and intensity of the storm are implemented using functions of past values and other variables including a random component. Modifications are based on statistics of historical storms in that area of the ocean (or over land). The circulation of the storm is obtained by computational fluid dynamics solutions to the equations for fluid motion using a 2-dimensional simulation that is a function of storm radius to maximum winds, a storm shape parameter known as Holland B, and speed of forward travel of the storm. A set of solutions is pre-calculated for use during the storm simulations. As a storm passes near a point of interest, the speed and direction of speeds at various directions is recorded. Simulation of many thousands of storms then yields a statistically valid simulation.

Figure 6 shows two simulated hurricane tracks in the Eastern Pacific in comparison to actual historical storms. The storm tracks are generated beginning at the same locations as historical storms, because there is insufficient knowledge of storm genesis to simulate that aspect. The simulated tracks have a random character in speed, direction and strength (rotational speed) to intentionally generate different storm tracks and storm characteristics. In Figure 6, the blue storms are historic, while the simulated storm colors represent sea surface temperature and the size represents intensity.

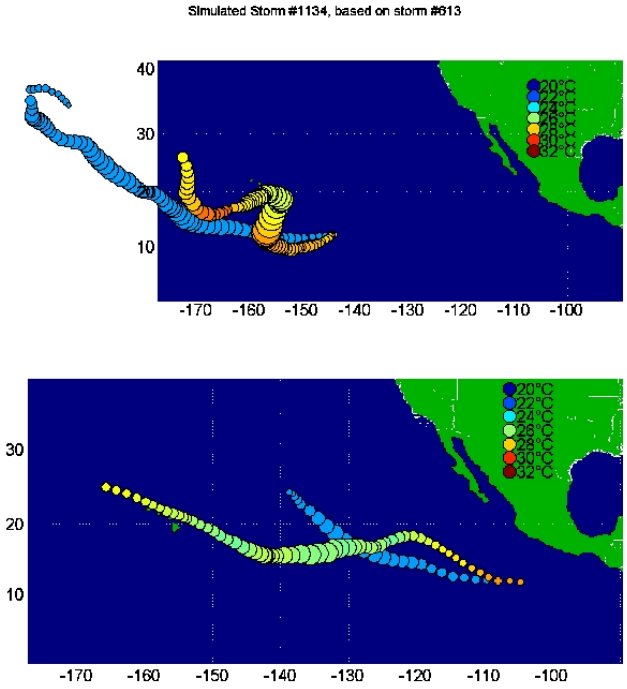

Figure 6: Historical v. Simulated Tracks.

In Figure 6, the bottom image replicates a typical storm track (but intentionally not exactly the original). In the upper image, a high-intensity storm makes a right turn, traveling rapidly north into cooler water without the reduction in intensity associated with cooler water that would occur if the speed of travel were lower. This is the type of storm motion that has produced major hurricanes in Hawaii.

Hundreds of thousands of storms and tracks are generated for a simulation. In order to know the speed and direction at any location near a storm track, a storm rotational model is

applied at each location of the storm. Figure 7 shows rotational characteristics for a few cases obtained from the solution of the differential equations of motion for specific variables.

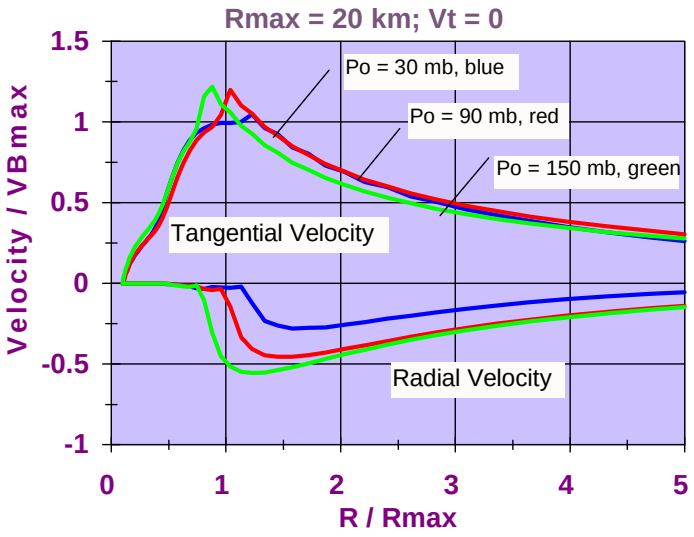

Figure 7: Rotational Wind Field Example.

Validation of the Monte Carlo method for hurricanes requires that the model be able to reproduce historical meteorological data at ground or buoy stations. Figures 8a to 8c show one such match obtained by running the model over an actual hurricane path with hurricane properties inserted into the model. Gust speed, mean speed and wind direction at a physical anemometer location are compared to the simulation as a function of time during the storm. For multiple anemometer measurement locations for a single storm, the simulation should reasonably match data at all measured meteorological stations.

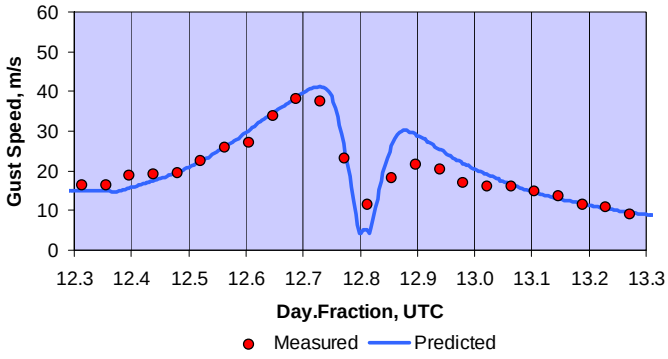

Figure 8a: Gust speed simulation for a hurricane.

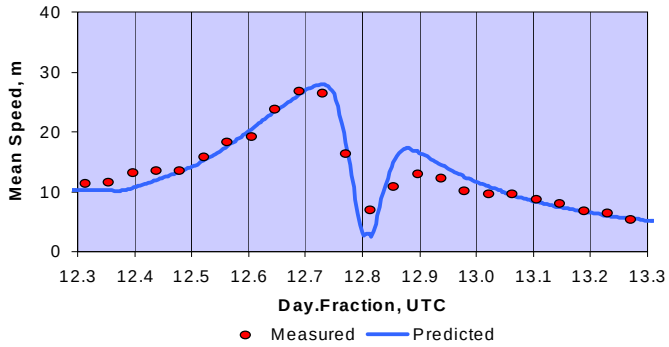

Figure 8b: Mean speed simulation for a hurricane.

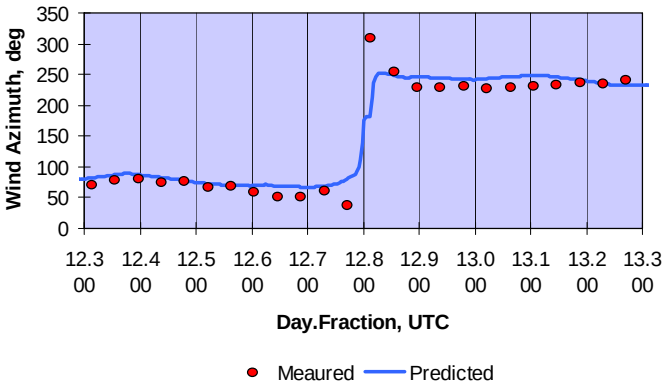

Figure 8c: Direction simulation for a hurricane.

Figure 9 shows contours of storm frequency in the Eastern Pacific for hurricane simulations in comparison to measured data. The colors represent the number of hurricane force storms within a 75 NMi radius per 10 years. Note the uneven character near the Hawaiian Islands for the actual storms recorded. The high variability is a result of sampling error (i.e. variability due to a small sample size) and is caused by the short data record. The smoother contours in the lower image are due to the hundreds of thousands of storms used in the simulation (i.e. a large sample size). In other words, the lack of hurricanes in the eastern Hawaiian Islands in recent history is a random occurrence and should not be expected to continue.

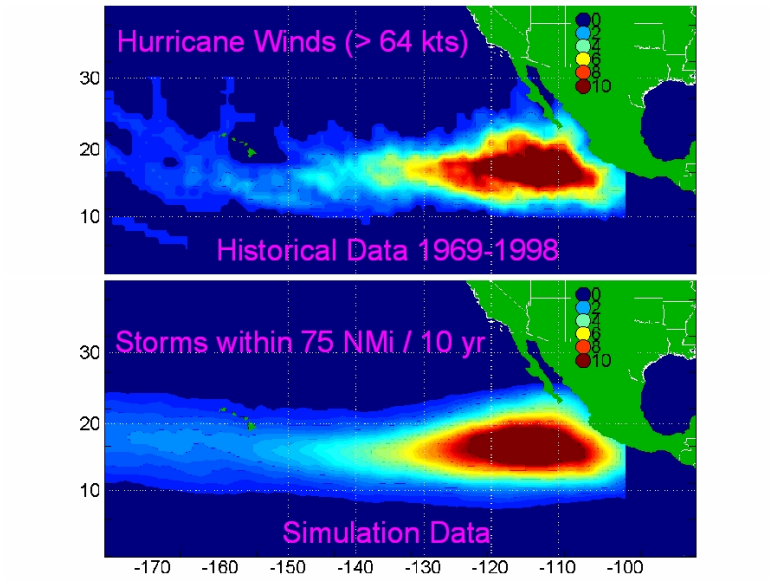

Figure 9: Historical v. Simulated Occurrence.

Tornados

Tornados are not explicitly included in the design of structures under ASCE 7, including effects of debris impact and rapidly changing load magnitude and direction. With respect to speed, since about half of all tornados have peak speeds less than about 50 mps (about 100 mph), and since the 3-second wind speeds associated with strength design (LRFD factored loads) are about 51 mps (114 mph) in the major wind-field areas of the central US, structures designed and constructed in conformance with ASCE 7 may withstand about half of all tornados (F0 and F1).

To illustrate the risk of tornados, a simulation was performed for a hypothetical wind farm in the mid-west. The simulation was performed utilizing a Monte Carlo model developed from 56 years of tornado data. Note that this data utilized the Fujita (F) scale for intensity, and did not include data reported in the recently implemented Enhanced Fujita (EF) scale. The Monte Carlo method was used to generate a 100,000 year record of tornados to obtain statistically significant results.

The hypothetical wind farm consisted of 100 turbines. It was assumed that the effective area of each turbine was 4537m^2 based on a 38m rotor radius. The turbines were set in a configuration of 4 rows of 25. Each row was 1000m apart, while each turbine within a row was spaced 300m apart. This resulted in a total wind farm effective area of roughly 22.4km^2, see Figure 10.

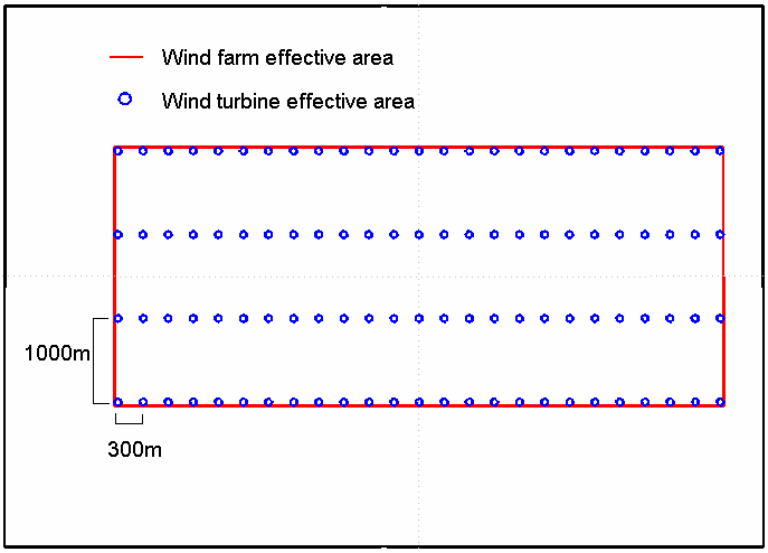

Figure 10: Hypothetical wind farm configuration.

Figure 11 shows tornado tracks for a 1,000 year period from the 100,000 year simulation. In general, the wider tracks represent stronger tornados, but that was not necessarily the case every time. Some tornados do not hit any turbines, while the larger ones hit several. Figure 12 shows the number of tornado hits to the gross area of the farm per 100 years (left), while the right image shows the percent of the total farm area impacted by tornados. The maximum area was hit by F2 tornados, because the smaller F values have more hits but smaller areas, while the larger F number tornados have a wide path when they occur but are much less likely. Figure 13 shows the same information, but for the area occupied by turbines – i.e. these are direct hits on individual turbines. Again the F2 tornados have the most impact. For an ASCE 7 compliant design, F2, F3 and F4 are damaging tornados.

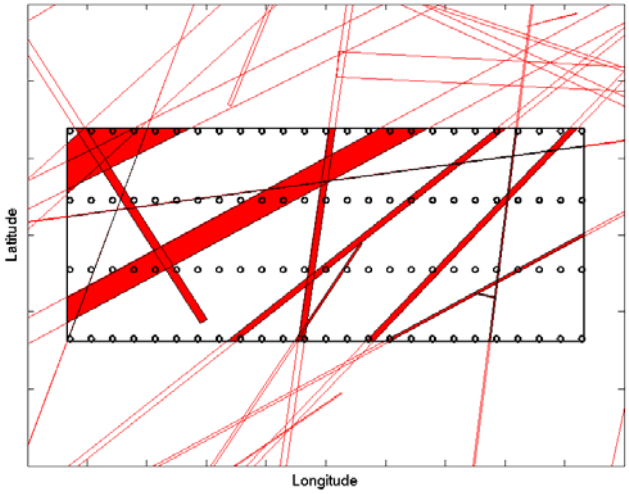

Figure 11: Simulated tornado tracks from a 1,000 year period to exemplify impact.

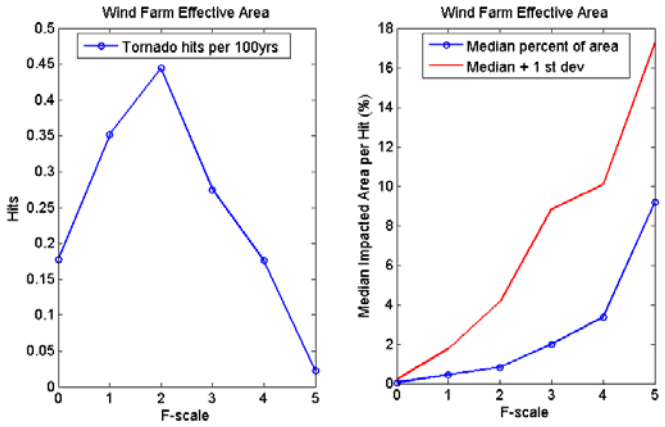

Figure 12: Tornado impacts on the total effective area of the wind farm.

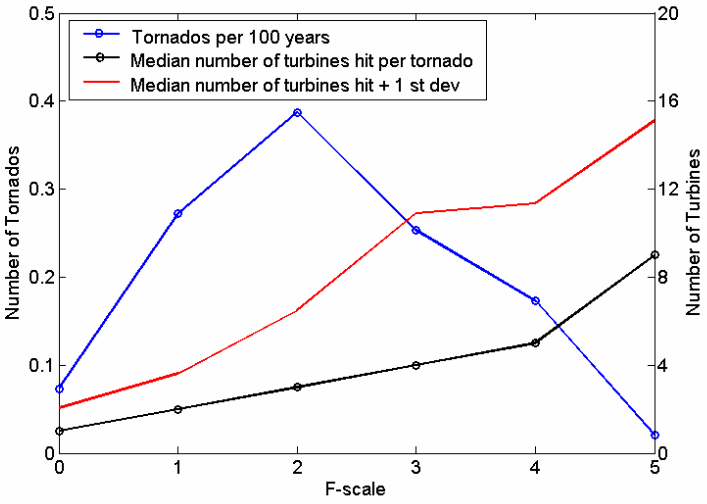

Figure 13: Tornado impacts on the effective areas of the turbines.

The wind farm as a single entity was impacted by 1,445 tornados over the 100,000 year simulation, suggesting a return period of roughly 70 years (110 years for F2 or stronger). A total 1,179 (or 82%) of the tornados actually impacted specific turbines. The turbines themselves were hit 5,042 times by these 1,179 tornados. This indicates that over 75% of the time one tornado impacts multiple turbines. The results also indicate that at least one turbine will be hit every 20 years (25 years for F2 or greater). This methodology provides a means to quantitatively evaluate tornado risks to wind turbine farms.

Fatigue Issues

For most structures, Load Factors (LRFD) or Safety Factors (Allowable Stress) are used to set the reliability level, so that a design event (first yield, buckling failure, etc.) is set to occur for a sufficiently extreme event that personnel safety and project economics are not compromised. One issue in defining the design load for wind turbines is that fatigue loading may play an important role, unlike typical buildings where fatigue in the building frame is usually insignificant. In wind loading, fatigue can be a narrow band (near-single frequency) or broadband process (wide spectrum of frequencies where a fundamental frequency may not be

easily observed in a plotted time series of the load). In either case, a mean stress can accompany the fatigue cycling. In a broadband process, counting stress cycles may not be obvious where a natural frequency in the structure is not excited discretely. A rain-flow cycle counting algorithm (Xu et al, 1995) can be useful to determine the matrix of cycle count and mean stress offset.

Figure 14 shows a small portion of a time series of load to illustrate the cycle counting algorithm of Xu. The time series starts with the largest positive (negative works also) load (or stress). The first cycle moves negatively as far as possible, jumping over intermediate smaller oscillations; then reverses at the most negative location, and progressing in a positive direction until the original level is reached. Other cycles are defined using unused segments of the signal. Some cycles are positive-negative-positive, while others are negative-positive-negative. The process continues until all parts of the time series is exhausted. A computer program can easily be taught this algorithm.

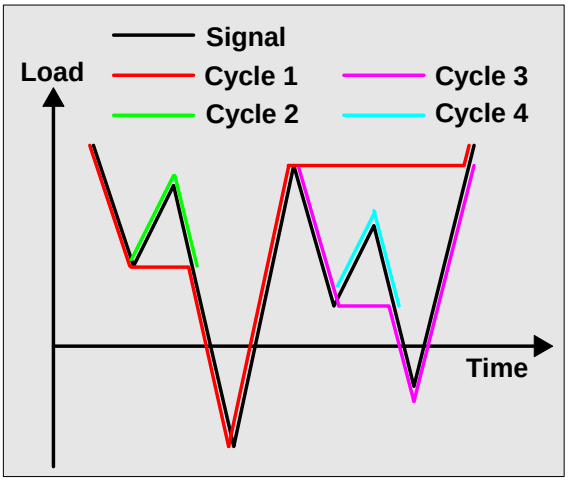

Figure 14: Rainflow cycle counting method for a broadband process.

The total number of cycles, range (most positive value minus most negative value), and mean (half way between these two extremes) can be plotted as shown in Figure 15 for each structural member under evaluation. This type of analysis provides a method for accumulating fatigue damage from a theoretical model or provides guidance for design of a fatigue experiment.

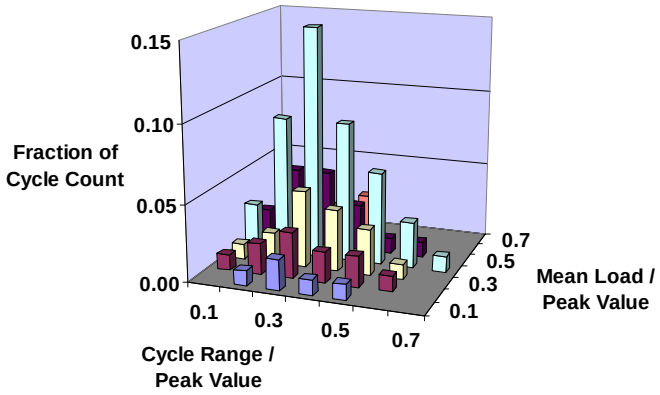

Figure 15: Cycle counts as a function of mean load and load range.

Conclusions

Several wind load design issues were presented and discussed relative to wind farms, some of which differ from procedures in international standards. ASCE 7, the US national wind load standard was used as a model for wind load development, but some topics were identified where somewhat different approaches might be taken.

References

ASCE, American Society of Civil Engineers (2006), Minimum Design Loads for Buildings and Other Structures (ASCE 7-05).

ASCE, American Society of Civil Engineers (1999), Wind Tunnel Model Studies of Buildings and Structures (ASCE Manual of Practice Number 67).

Banks, D. and J.A. Peterka (2001), Tropical Storm Track Prediction Using Autoregressive Time Series Analysis, Americas Conference on Wind Engineering, Clemson University.

Cermak, J.E. (1971), "Laboratory Simulation of the Atmospheric Boundary Layer," *AIAA Jl.*, Vol. 9, September.

Cermak, J.E. (1975), "Applications of Fluid Mechanics to Wind Engineering," A Freeman Scholar Lecture, *ASME Journal of Fluids Engineering*, Vol. 97, No. 1, March.

Chay, M.T. , F. Albermani, R. Wilson. (2006), Numerical and Analytical Simulation of Downburst Wind Loads, *Engineering Structures* Vol. 28, pp240–254.

Chock, Gary, Peterka Jon, and Yu, Guangren (2005), Topographic Wind Effects and Directionality Factors for Use in the City & County of Honolulu Building Code, 10th Americas Conference on Wind Engineering, Louisiana State University, Baton Rouge.

ESDU (1993a) Strong Winds in the Atmospheric Boundary Layer, Part 1: Mean Hourly Wind Speeds, ESDU Report 82026, ESDU International.

ESDU (1993b) Strong Winds in the Atmospheric Boundary Layer, Part 2: Discrete Gust Speeds, ESDU Report 83045, ESDU International.

Orwig, K.D. and J.L. Schroeder (2007), "Near-Surface Wind Characteristics of Extreme Thunderstorm Outflows," *J. Wind Eng. and Ind. Aero.*, Vol. 95, pp. 565-584.

Peterka, J.A. (1992), "Improved Extreme Wind Prediction for the United States," *J. Wind Eng. and Ind. Aero.*, Vol. 41, pp. 533-541.

Peterka, J.A. and Shahid, S. (1998), "Design gust Wind Speeds for the U.S.," *ASCE Journal of Structural Engineering*, Vol. 124, pp. 207-214.

Peterka, J. A. and David Banks (2002), Wind Speed Mapping of Hawaii and Pacific Insular States by Monte Carlo Simulation, Report for NASA Contract NASW-99046, NASA Goddard Space Flight Center, CPP Inc. Project 99-1773.

Twisdale, L.A. and Vickery, P.J. (1993), "Uncertainties in the Prediction of Hurricane Windspeeds," Proceedings of *Hurricanes of 1992*, ASCE, pp. 706-715, December.

Vickery, P.J., Skerlj, P.F., Steckley, A.C. and Twisdale, L.A. (2000a), "Hurricane Wind Field Model for Use in Hurricane Simulations," *ASCE Journal of Structural Engineering*, Vol. 126 No. 10, pp. 1203-1221.

Vickery, P.J., Skerlj, P.F. and Twisdale, L.A. (2000b), "Simulation of Hurricane Risk in the U.S. Using Empirical Track Model," *ASCE Journal of Structural Engineering*, Vol. 126 No. 10, pp. 1222-1237.

Xu, Y.L., Mehta, K.C. and G.F Reardon (1995), Fatigue of Metal Roof Cladding Subject to Wind loading, Part I: Fatigue-Related Characteristics of Roof Pressures, Proceedings, Ninth International Conference on Wind Engineering, City, New Delhi, India, pg 1067-1078.